HAL
open science

Direct observation of oxygen superstructures in manganites

Stéphane Grenier, K.J. Thomas, J.P. Hill, U. Staub, Y. Bodenthin, M. Garcia-Fernandez, V. Scagnoli, V. Kiryukhin, S.-W. Cheong, B.G. Kim, et al.

To cite this version:

Stéphane Grenier, K.J. Thomas, J.P. Hill, U. Staub, Y. Bodenthin, et al.. Direct observation of oxygen superstructures in manganites. Physical Review Letters, 2007, 99, pp.206403. 10.1103/PhysRevLett.99.206403 . hal-00149105v2

HAL Id: hal-00149105

https://hal.science/hal-00149105v2

Submitted on 16 Nov 2007

HAL is a multi-disciplinary open access archive for the deposit and dissemination of scientific research documents, whether they are published or not. The documents may come from teaching and research institutions in France or abroad, or from public or private research centers.

L'archive ouverte pluridisciplinaire **HAL**, est destinée au dépôt et à la diffusion de documents scientifiques de niveau recherche, publiés ou non, émanant des établissements d'enseignement et de recherche français ou étrangers, des laboratoires publics ou privés.

Direct observation of oxygen superstructures in manganites

S. Grenier,[1] K. J. Thomas,[2] J. P. Hill,[2] U. Staub,[3] Y. Bodenthin,[3] M. García-Fernández,[3] V. Scagnoli,[4] V. Kiryukhin,[5] S-W. Cheong,[5] B. G. Kim,[5,*] and J. M. Tonnerre[1]

[1] *Institut Néel, CNRS & Université Joseph Fourier, BP 166, F-38042 Grenoble Cedex 9, France*
[2] *Condensed Matter Physics and Materials Science Dept., Brookhaven National Laboratory, Upton, New York 11973, USA*
[3] *Swiss Light Source, Paul Sherrer Institut, 5232 Villigen, Switzerland*
[4] *European Synchrotron Radiation Facility, BP 220, F-38043 Grenoble Cedex 9, France*
[5] *Department of Physics and Astronomy, Rutgers University, Piscataway, New Jersey 08854 USA*

(Dated: November 16, 2007)

We report the observation of superstructures associated with the oxygen $2p$-states in two prototypical manganites using x-ray diffraction at the oxygen K-edge. In the stripe order system $Bi_{0.31}Ca_{0.69}MnO_3$, hole-doped O states are orbitally ordered, at the same propagation vector as the Mn orbital ordering, but no oxygen charge stripes are found at this periodicity. In $La_{\frac{7}{8}}Sr_{\frac{1}{8}}MnO_3$, we observe a $2p$ charge ordering described by alternating hole-poor and hole-rich MnO planes that is consistent with some of recent predictions.

Fascinating macroscopic properties may emerge from the electronic and magnetic orderings in doped $3d$ metal oxides. In cuprates, charge and spin stripes could be relevant to high-T_C superconductivity [1] whereas the colossal magnetoresistance in manganites is fundamentally related to the stability of the correlated orderings of polarons, charges, orbitals and spins [2]. The relationship between the orderings and the transport properties has been adressed both theoretically and experimentally focusing on the $3d$ metal atoms, often neglecting the ligands' degrees of freedom. However, the active states are not ionic $3d$ metal orbitals, but, rather hybridized metal $3d$ - oxygen $2p$ states, therefore an ordering of the oxygens must equivalently accompany an ordering of the metals. In cuprates, the role of the oxygen atom is now always considered and, taking a recent example, the ordering of hole-doped oxygens was directly observed and discussed in the context of the stripes [3].

In manganites, an electronic ordering on oxygens has not been detected yet, although recent experiments have suggested a crucial role of the O atoms in the correlated orderings on Mn atoms. X-ray spectroscopy of Mn atoms has revealed a small charge disproportionation, emphasizing the inadequacy of the traditional model of strongly localized charge ordering (Mn^{4+}/Mn^{3+}) [4]. The conductivity was also found related to the oxygen electronic configuration [5], and it was proposed that the oxygen atom bridges an electron between two Mn atoms of nearly the same valence, coupling them magnetically [6]. Actually, these results point out the role of the $2p-3d$ hybridization in determining the magnetic exchange couplings and conductivity, the traditional picture being the one where the atomic $3d$ orbitals define exchange magnetic pathways between Mn atoms, the oxygen $2p$ states being filled.

Meanwhile, new theoretical models beyond the Mn-centered description also suggested that oxygen superstructures play an important role in determining the ground states. Ferrari *et al.* [7] explained the insulating behavior of the charge/orbitally orded half-doped system by an ordering of O holes - "oxygen stripes" of varying valences (incidentally, having the same periodicity as the Mn orbital ordering). Efremov *et al.* [8] proposed that the charge ordering could correspond to a charge density wave (CDW) that is either Mn-centered or O-centered, and that an intermediate CDW (an intermediate O-Mn charge transfer) would potentially give both ferromagnetism and ferroelectricity. Also, Volja *et al.* [9] insisted on the relevance of the Mn charge ordering concept, if the hybridization with the hole-doped O atoms is properly considered.

Experiments that directly probe the oxygen contribution to the ordered states provide essential feedback to these theoretical models. In this Letter, we show that O K-edge resonant diffraction spectra reveal the oxygen superstructures in manganites. We first report the direct observation of the *orbital* ordering of hole-doped, hybridized, O $2p$-states in a Mn-centered, Mn-orbitally ordered manganite, $Bi_{1-x}Ca_xMnO_3$ ($x = 0.69$). Second, we report the *charge* ordering on the oxygen in $La_{\frac{7}{8}}Sr_{\frac{1}{8}}MnO_3$; our observations confirm the stacking of alternate hole-rich and hole-poor planes. In both cases, the O states are directly related to the Mn states, emphasizing the hybridized nature of the active states involved in the electronic orderings.

$Bi_{0.31}Ca_{0.69}MnO_3$ (BCMO) is representative of the Mn-centered orbitally ordered CDW phase, which is usually described as Mn stripe order. This phase is robust in manganites, from half-doping to $x = 0.8$ [2]. The CDW exhibits polaronic sites (Mn^{3+}) placed as far as possible from each other, with an antiferro order of the valence orbital, while Mn^{4+} sites are isotropic [10] (Fig. 1). As the doping increases, the polaron density diminishes, and a larger orbital ordering periodicity is obtained ($\Lambda \approx 17$ Å for BCMO), which is large enough to diffract soft x-rays near the O K-edge ($\lambda = 23.4$ Å at 530 eV). BCMO orders below $T_{OO} = 250$ K. The second system, $La_{\frac{7}{8}}Sr_{\frac{1}{8}}MnO_3$

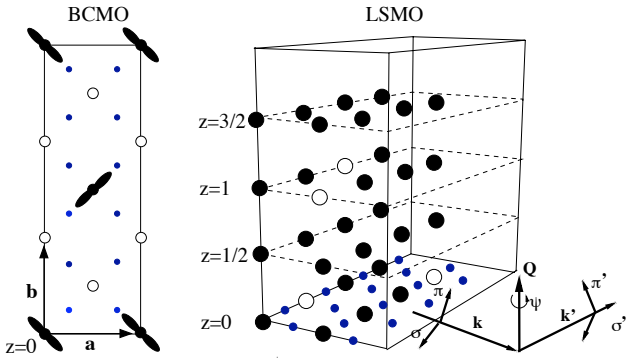

FIG. 1: Simplified orderings in BCMO and LSMO. Closed circles represents polaronic Mn^{3+} atoms, open circle are Mn^{4+} and small circles are the O sites; the orbital ordering in BCMO is also shown. The structure in the a-b plane of BCMO repeats in adjacent planes, while LSMO planes alternate between being hole-rich (z=0 and 1) and hole-poor (z=1/2 and 3/2) [11]; for clarity the oxygens are represented in the first plane only. The scattering geometry is indicated, ψ is the azimuthal angle, σ and π are the two polarization components.

(LSMO), exhibits several phase transitions upon cooling. At $T_{OO1} \approx 280$ K, a polaronic insulating orbital ordering takes place. Then, the system becomes a metallic ferromagnet at $T_C \approx 180$ K but finally stabilizes below $T_{OO2} \approx 150$ K as an insulating ferromagnet. It was recently demonstrated that the OO1 to OO2 transition corresponds to a rearrangement of the polarons in a larger unit cell [11]. Here, we directly probed the electronic ordering that accompanies the polaron rearrangement allowing the test of two recent models for the electronic structures (described below).

The BCMO compound was prepared by the flux technique and LSMO by the floating zone technique; both samples were characterized by hard x-ray diffraction. The crystals were cut and polished with the normal to the surface along [010] for BCMO, and along [001] for LSMO. We refer to the P*bnm* orthorhombic notations for the unit cell.

The data were collected at the SIM beamline of the Swiss Light Source using the RESOXS set-up built for soft x-ray diffraction and reflectivity in ultra high vacuum [12]. The experiments were performed as in conventional diffraction but with the incident energy varied through the O K-edge whilst moving the diffractometer angles to maintain the diffraction condition. The O K-edge corresponds to the photoelectric transition of a $1s$ electron to unoccupied orbitals ψ_n. This transition is accounted for in the scattering factor by the overlap integral $\hat{\varepsilon}\cdot\int \psi_n^*(\mathbf{r})\mathbf{r}\psi_{1s}^{\mathrm{O}}(\mathbf{r})d\mathbf{r}$, $\hat{\varepsilon}$ being the photon polarization. The resonant and the Thomson scattering factors are then weighted by the crystallographic phase-factor at the selected Bragg reflection, $F(Q,\omega) = \sum_j f_j(Q,\omega)e^{i\mathbf{Q}\cdot\mathbf{r}_j}$, ω being the energy of the photon and the energy between ψ_n and ψ_{1s}^{O} [13]. By sweeping the incident photon energy through the O K-edge, a resonant reflection provides evidence of the periodicity of unoccupied states ψ_n from and above the Fermi level (ε_f). The states probed are those without an even symmetry relatively to the oxygen $1s$ orbital ψ_{1s}^{O} (which is even), as easily seen from the overlap integral. Near ε_f, those may be O $2p$'s, or orbitals from nearby atoms with some projection on the oxygens (*e.g.* $3d$), or orbitals made of a hybridization of the two. Farther above ε_f, the states are more delocalized and may not carry an information on the electronic structure but rather on all surrounding atoms, *i.e.* a structural information. We also measured azimuthal scans (record of the reflection intensity while rotating the crystal in a plane normal to $\mathbf{Q}$) which allow one to rotate the polarization of the photon relatively to the atoms thereby probing different directions of the unoccupied states (ψ_{2p_x},...). We could select the two incident polarizations, namely σ or π, perpendicular to and within the scattering plane, respectively (Fig. 1), the detector integrating photons of both polarizations.

Fig. 2a shows the O K-edge RXD spectrum at the (0 0.31 0) superstructure reflection we found in BCMO, for π and σ incident polarizations. No scattering is observed outside a narrow energy range (1.1 eV) at the edge of the absorption spectrum (given by the fluorescence yield). We observed equal spectra for the two incident polarizations. As has been discussed elsewhere [10] this implies that the scattering process is one in which the polarization of the photon is rotated, of the type $\sigma \rightarrow \pi$ or $\pi \rightarrow \sigma$, that is, with zero $\sigma \rightarrow \sigma$ and $\pi \rightarrow \pi$ scattering. The incommensurability of this reflection is observed to vary with temperature, stabilizing at about 0.31 r.l.u., below T_{OO} (Fig. 2b). A final observation, from Fig. 2c, is the extinction of the reflection when the polarization of the incident photon is perpendicular to the ordered (a, b) plane.

The first observation indicates a resonant superstructure reflection from an ordering of the very first unoccupied states from ε_f projected on the O atoms (ψ_{1s}^{O}), with the propagation $Q = 0.31$ r.l.u, corresponding to the periodicity of the Mn orbital ordering [10]. Following earlier analysis of the absorption data [14], the comparison with the fluorescence yield allows us to identify the ordered states as the $2p$ states hybridized with the $3d$. The narrow spectral width observed reflects the width of the (unoccupied) hybridized band. The second observation demonstrates that there is no charge ordering on O atoms *at this wave vector*. Indeed, a CDW of this periodicity would scatter in the $\sigma \rightarrow \sigma$ channels, which is absent on this reflection to within the uncertainty of our measurements. Furthermore, a charge order scatters at all azimuthal angles [15, 16], at odds with the data. These three observations prove that the O $2p$ states are hole-doped and show orbital ordering, and not charge ordering at this propagation vector. Therefore, the data exclude a direct extension of the model of oxygen stripes, with the

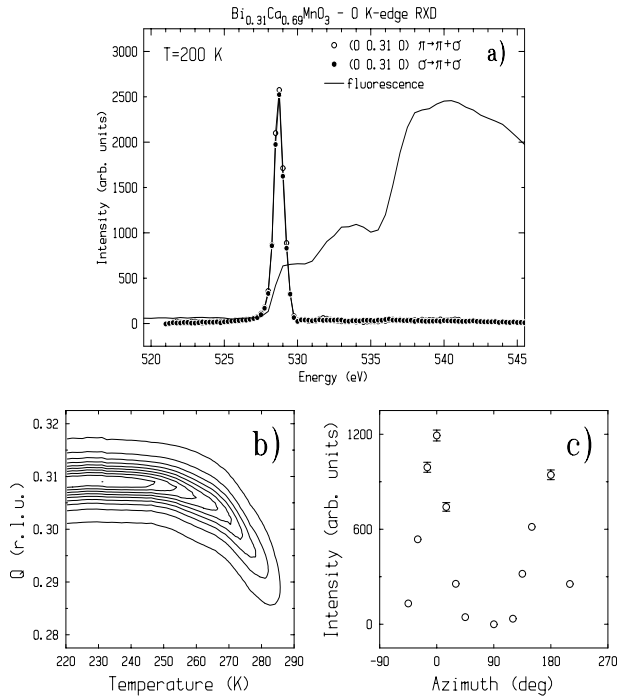

FIG. 2: a) The (0 0.31 0) superstructure reflection, corrected from fluorescence but not for self-absorption; nevertheless, the intensity is zero off the O K-edge. b) Temperature dependence of the peak position at the phase transition. c) Azimuthal dependence displaying a two-fold symmetry with a maximum with the incident polarization along **a**, and zero along **c**, taken at 528.75 eV, T=200K.

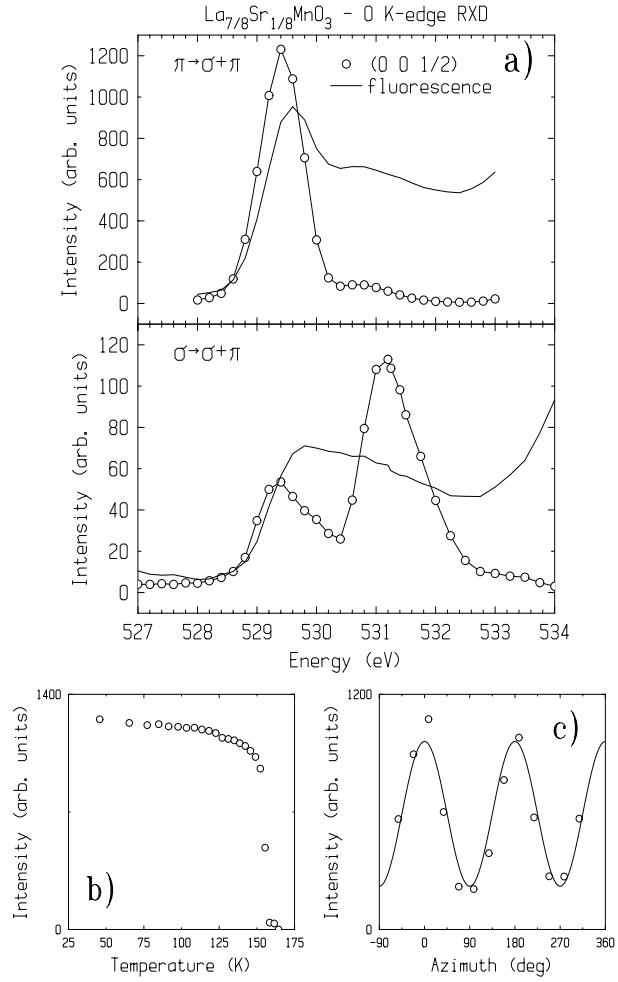

FIG. 3: a) RXD spectra of the $(00\frac{1}{2})$ reflection at the O K-edge of $La_{\frac{7}{8}}Sr_{\frac{1}{8}}MnO_3$, with two incident polarizations, $T = 30$ K. $\psi \approx 90°$. b) Temperature dependence of the reflection. c) Azimuthal dependence at 529.2 eV, $\sigma \rightarrow \sigma + \pi$ channels, compared to a $\cos^2$ +const. function (solid line), 0° is σ incident polarization along **b**, 90° along **a**.

periodicity of the Mn orbital ordering, from half-doping [7] to this high doping.

The observation of $2p$ orbital ordering makes intuitive sense in light of the $2p-3d$ hybridization and the earlier observation of this same orbital ordering, but projected on the Mn atoms (ψ_{2p}), at the Mn $2p \leftrightarrow 3d$ L-edge [10]. Specifically, these states are centered on the polaronic Mn atoms, with a configuration depicted in Ref. [9, 17] clearly exhibiting the unoccupied $2p$ ordering on the four O surrounding the polaronic Mn. In agreement with this model, our results demonstrate the charge transfer nature of the compound and the coupling between the O and Mn orbital ordering.

We now turn to $La_{\frac{7}{8}}Sr_{\frac{1}{8}}MnO_3$. Fig. 3a shows the RXD spectra of the $(00\frac{1}{2})$ superstructure reflection at the O K-edge for two incident polarizations. Previous studies have already reported the unusual stacking that doubles the unit cell along **c** below T_{OO2} [18]; the present data also reveals a specific $2p$-state reordering (Fig. 3a and b). The fluorescence yields (proportional to $\Im m f$) and the RXD spectra are different for the two polarizations, the differences provide evidence of an anisotropy of the unoccupied O states near ε_f. The main characteristic of the $2p$ ordering is identified by considering the azimuthal dependence of the reflection. The azimuthal scan never goes to zero; it has a $\cos^2 +$ const dependence (Fig. 3c). A tensorial analysis of the resonant scattering permits to easily identify the origin of the two terms [16]: The constant term is due to a net difference in the total charge carried by the oxygens on different planes, whereas the sinusoidal dependence is due to the relative direction of the polarization of the photon with the anisotropic O electronic structure.

The diffraction vector $(0\ 0\ \frac{1}{2})$ corresponds to the net difference in scattering, hence to a net difference in holes, from planes separated by $\Delta z = 1$; a charge ordering at the $(0\ 0\ \frac{1}{2})$ vector provides a strong constraint to the theoretical models for the charge ordering pattern. The models by Korotin *et al.* [19] and by Geck *et al.* [11] both propose that hole-rich and hole-poor Mn planes alternates along **c** but with different stacking orders. In

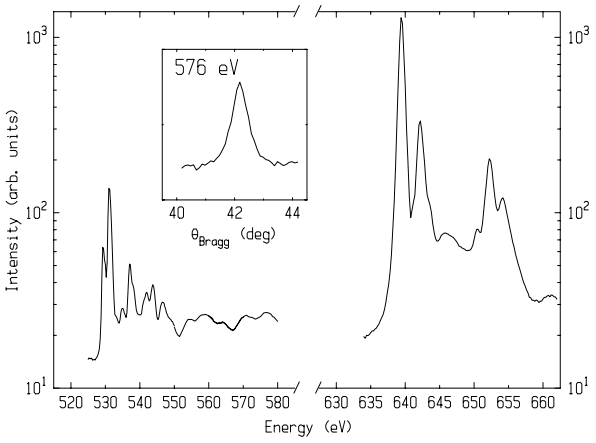

FIG. 4: RXD spectrum of the $(00\frac{1}{2})$ reflection of $La_{\frac{7}{8}}Sr_{\frac{1}{8}}MnO_3$, $\sigma \rightarrow \sigma + \pi$ channels, $T = 30$ K. The O near-edge (≈ 530 eV) and the Mn $L_{III/II}$-edges (≈ 640 and ≈ 652 eV) probe the active states near ε_f, while the region between 535 and 560 eV correspond to states that are delocalized (high energy from ε_f). Inset shows the diffraction peak at 576 eV, emphasizing the existence of the reflection far above the edge.

Geck's model every other planes are identical when projected on the **c** axis: they should not give the charge order scattering we observe. In Korotin's model, three successive hole-rich planes alternate with one hole-poor plane. Such order should give rise to a strong charge order signal on the O atoms because of the hybridization, as we observe. We note that only Geck's model explains reflections with a planar component observed elsewhere [11].

Scattering is observed at this wave-vector for energies well above the O K-edge (Fig. 4). Increasing the energy from the near-edge, the photoelectron probes states that are more delocalized, thus more sensitive to the crystal structure due to band structure effects. These features signal presence of lattice distortions accomodating the charge ordering on oxygen atoms. At higher energy, the Mn L-edges correspond to the direct probe of the states nearby ε_f, like the O near-edge, but probed by the Mn $2p$ electrons and thus projected on the Mn atoms. Some of the near ε_f hybridized states are probed at both edge, projected on O and Mn, respectively. The intensities at both near-edges in Fig. 4 provide the relative scattering strength of each atoms which should help determine the hybridization, charge transfer and overlap, between the O and Mn orbitals.

In conclusion, resonant x-ray diffraction at the O K-edge has been used to detect the electronic superstructures of the $2p$ states near ε_f in two manganites. In $Bi_{0.31}Ca_{0.69}MnO_3$, we show evidence of an orbital ordering of hole-doped hybridized $2p - 3d$, and contradict O charge stripes with the same propagation vector as the Mn orbital ordering. In $La_{\frac{7}{8}}Sr_{\frac{1}{8}}MnO_3$, the data provided evidence of a charge ordering on the O atoms with the $(0\ 0\ \frac{1}{2})$ propagation vector, corresponding to a specific plane stacking with differing hole concentrations. The orderings on O atoms are not experimentally dissociated from the orderings on the Mn atoms, in both compound, emphasizing the hybridized nature of the orbitals near ε_f. Quantification of the hole densities and of the $2p-3d$ hybridization requires *ab initio* calculations of the ground state and the excited state using dedicated formalisms (the excited state has a strong Coulomb potential in a core shell and an extra electron in the valence shell). The RXD technique can also be chemically-sensitive to the magnetic moment, therefore these results suggest potential measurements of magnetic superstructures on the oxygens. Thus, the RXD data open a view on the $2p-3d$ states, the magnetic exchange couplings between $3d$ metals and on the electronic superstructures at play in this strongly correlated system.

We benefitted from the excellent support of the staff on X11MA-SLS, PSI. M.G.-F. thanks the Swiss National Science Foundation. This work was also supported by US Dept of Energy, Division of Materials Science, under contract No. DE-AC02-98CH10886. We thank J. Debray and S. Garaudée of the Institut Néel for excellent technical assistance.

* Department of Physics, Pusan National University, Pusan 609-735, Korea

[1] J. M. Tranquada, et al., Nature **375**, 561 (1995).
[2] T. Chatterji, ed., *Colossal Magnetoresistive Manganites* (Kluwer, Dordrecht, 2004).
[3] A. Rusydi, et al., Phys. Rev. Lett. **97**, 016403 (2006).
[4] G. Subías, et al., Phys. Rev. B **56**, 8183 (1997).
[5] M. Abbate, et al., Phys. Rev. B **46**, 4511 (1992).
[6] A. Daoud-Aladine, et al., Phys. Rev. Lett. **89**, 097205 (2002).
[7] V. Ferrari, et al., Phys. Rev. Lett. **91**, 227202 (2003).
[8] D. V. Efremov, et al., Nature Materials **3**, 853 (2004).
[9] D. Volja, et al., cond-mat:0704.1834v1 (2007).
[10] S. Grenier, et al., Phys. Rev. B **75**, 085101 (2007).
[11] J. Geck, et al., Phys. Rev. Lett. **95**, 236401 (2005).
[12] N. Jaouen, et al., Journal of Synchrotron Radiation **11**, 363 (2004).
[13] *Resonant Anomalous X-Ray Scattering, Theory and Applications* (Materlik, Sparks and Fisher, 1994).
[14] H. L. Ju, et al., Phys. Rev. Lett. **79**, 3230 (1997).
[15] J. García, et al., J.Phys. Cond. Matt. **13**, 3243 (2001).
[16] S. Grenier, et al., Phys. Rev. B **69**, 134419 (2004).
[17] W.-G. Yin, et al., Phys. Rev. Lett. **96**, 116405 (2006).
[18] Y. Yamada, et al., Phys. Rev. Lett. **77**, 904 (1996).
[19] M. Korotin, et al., Phys. Rev. B **62**, 5696 (2000).